This article has been accepted for publication in a future issue of this journal, but has not been fully edited. Content may change prior to final publication. Citation information: DOI 10.1109/LAWP.2018.2873898, IEEE Antennas and Wireless Propagation Letters

Reconfigurable Phased Array Antenna Consisting of High-gain High-Tilt Circularly Polarized Four-arm Curl elements for Near Horizon Scanning Satellite Applications

Hengyi Zhou, *Student Member IEEE*, Arpan Pal, *Member, IEEE,* Amit Mehta, *Senior Member, IEEE,* Hisamatsu Nakano, *Life Fellow,* Alessandro Modigliana, Thanos Arampatzis and Paul Howland

***Abstract*—A 2×2 phased array consisting of beam reconfigurable four-arm Right Handed Circularly Polarized (RHCP) curl unit elements antenna is presented. This array is designed at test frequency of 5.2 GHz and can undertake a high-gain near-the-horizon scanning with low grating lobes. Each curl antenna element has four ports and can provide four RHCP tilted-beams (θ = 48°) with a gain of 8.3 dBic. By switching the feeding ports, the curl element can reconfigure / switch these unit element beams in four different quadrants in space. The array exploits these high-gain high-tilt switchable beams for generating an extremely wide scanning range from -80° ≤ θ ≤ +80°. For the 2×2 array, in this range, the beam has a maximum gain of 12.4 dBic at θ = 40°. More importantly, the array provides RHCP beams with a gain of 10.5 dBic at near-the-horizon angles of θ ≈ 70° and provides a lower gain of 6.5 dBic in the zenith direction. This has promising applications in Communications On The Move (COTM) using Flat Panel Antenna (FPA) to Geosynchronous Orbit (GSO) satellites. Here, when operating at high latitudes require high-gain at near-the-horizon angles.**

***Index Terms*—Four-arm curl antenna, tilted beam, circularly polarized beam, array antenna, scanning range, near-the-horizon scanning.**

I. Introduction

Wide-angle scanning phased array antennas [1] are highly desirable in many civil, military, space and satellite applications, such as satellite phones and television [2], broadband internet services, radar systems [3] and intelligent transportation systems. However, scanning at near-the-horizon angles with high-gain by a conventional patch antenna array is difficult. This is due to the fact they have limited beam-width [4] and the beam directed in the zenith direction. In addition, the grating lobes increase significantly when conventional patch arrays scan at near-the-horizon angles, which further restrict the scanning range [5]. Similarly, a circularly polarized (CP) antenna array with a Butler matrix network also has been investigated for beam steering applications [6] [7]. These arrays can provide CP beam steering without phase shifters. However, they also only provide a limited scanning range and the gain still drops significantly at near-the-horizon angles.

To scan at near-the-horizon angles, various methods have been proposed [8-12]. However, the elements used for these methods only provide a linearly polarized beam. In addition, the main beam is zenith-pointing and thus the elements have a relatively lower gain at lower elevation angles. In recent years, pattern reconfigurable antennas [13]-[17] are gaining much attention to obtain a wide scanning range and provide a high gain at low elevation angles. In addition to the amplitude and phase for the excitation signal, these antennas can offer an additional (third) degree of freedom in the form of a reconfigurable element pattern. This extra degree of freedom enables an array of the reconfigurable antenna to achieve a wider scanning range by dividing the scanning space into multiple regions. In [18], an array of pattern switchable square loop antennas is demonstrated for a wide-angle scanning of −60° ≤ θ ≤ +60° with low grating lobes. However, the above-mentioned antennas [13]-[18] provide linearly polarized scanning beams. Therefore, these antennas are not suitable for satellite communication applications where circular polarization is required. This polarization limitation can be solved by using a circularly polarized switchable tilted high-gain antenna element [19].

In this paper, a 2×2 array composed of four-arm curl antennas, inspired from [19], is presented for near-the-horizon scanning with a circularly polarized high-gain high-tilt beam. The array antenna is designed for a test frequency of 5.2 GHz and can scan an upper elevation plane of −80° ≤ θ ≤ +80°,

Manuscript received XXXXXXXX; revised XXXXXXXXXXX; accepted XXXXXXXXXXXXX. Date of publication XXXXXXXXXXXXX; date of current version XXXXXXXXX

H. Zhou, A. Pal and A. Mehta are with the College of Engineering, Swansea University, Swansea SA1 8EN, U.K. (e-mail: 686785@swansea.ac.uk; a.pal@swansea.ac.uk; a.mehta@swansea.ac.uk).

H. Nakano is with the Science and Engineering Department, Hosei University, Koganei, Tokyo 184-8584, Japan (e-mail: hymat@hosei.ac.jp).

A. Modigliana and T. Arampatzis are with the Satellite Applications Catapult, Electron Building, Harwell Oxford OX11 0QR, UK (email: alessandro.modigliana@sa.catapult.org.uk; thanos.arampatzis@sa.catapult.org.uk)

P. Howland is with DSTL, CIS division, Salisbury SP4 0JQ, UK (email: pihowland@mail.dstl.gov.uk)

Color versions of one or more of the figures in this paper are available online at http://ieeexplore.ieee.org.

Digital Object Identifier XXXXXXXXXXX

which is a 30% improvement in the elevation scanning range, compared to that in [18]. More importantly, this array antenna is capable of providing a high gain at near-the-horizon angles and a relatively low gain in the axial direction without any additional circuits. Therefore, the proposed antenna is beneficial for Communications On The Move (COTM) using Flat Panel Antenna (FPA) with Geosynchronous Orbit (GSO) satellites for both land and UAV (Unmanned Aerial Vehicles) / drone terminals. Here the terminals require high-gain at near-the-horizon angle and low gain near the zenith when operating in high latitude regions.

II. 2×2 Array of Four-Arm Curl Antennas

Fig. 1 shows a 2×2 array composed of four-arm curl antennas. The four-arm curl element antenna is similar to the antenna presented in [19]. In this paper, the antenna is scaled from 1.575 GHz [19] to 5.2 GHz. The curl arm for this design is defined by Eg. (1).

$$r = Ae^{a\varphi} \tag{1}$$

The inner radial distance from the center to the starting point of each curl is A = 9.4 mm. The winding angle φ of the curl ranges from 0.5 to 1.13 rad and the curl constant is a = 0.125 rad^{-1}. The track width W of the antenna arm is 1.2 mm and the additional straight-line section L has a length of 1.5 mm. Each antenna arm is fed at the end of the additional straight-line section by an inner conductor of a coaxial line, having a diameter of 1.3 mm. Each antenna element (A, B, C or D) has four feeding ports, defined as A_i, B_i, C_i or D_i (i=1,2,3,4).

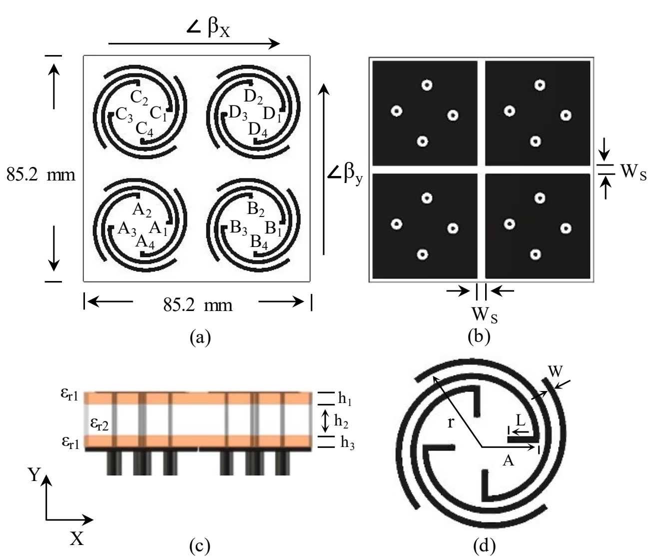

Fig. 1. The configuration of 2×2 array of four-arm curl antennas. (a) Top view. (b) Back view. (c) Side view. (d) Curl element configuration.

The array is printed on the top of a three-layered combined substrate. The upper and bottom substrate of RO3035 (relative permittivity ε_{r1} = 3.5 and loss tangent tan δ = 0.0015) has a thickness of $h_1 = h_3$ = 1.5 mm. A layer Delrin plastic (ε_{r2} = 3.4 and tan δ = 0.005) having a thickness of h_2 = 8 mm is inserted between the top and bottom layer. Hence, the antenna has a total height of $h_1+h_2+h_3$ = 11 mm (≈ 0.19λ_0, where λ_0 is the free-space wavelength at 5.2 GHz) as shown in Fig. 1(c). The overall planar size of the array is 85.2 mm (1.48λ_0) × 85.2 mm (1.48λ_0). The distance between two adjacent four-arm curl antenna elements is selected to be d = 0.74λ_0 at 5.2 GHz. As shown in Fig. 1(b), a slot having a width of W_S = 1.6 mm is introduced in the ground plane between two neighbouring antenna elements to obtain a wider CP beam. This is described in detail in the next section. Since each antenna element has four feeding ports, four antennas (A, B, C and D) in the 2×2 array has a total of 16 ports (A_1, A_2, A_3, A_4, B_1, B_2, B_3, B_4, C_1, C_2, C_3, C_4, D_1, D_2, D_3, and D_4).

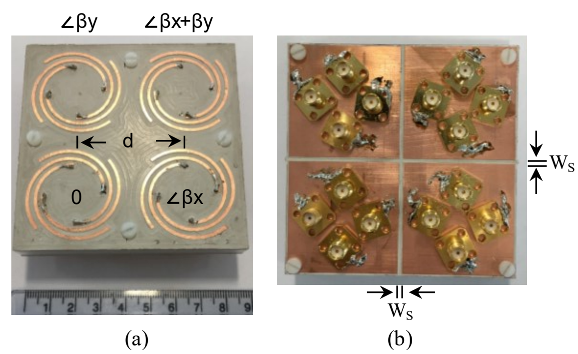

Fig. 2. Fabricated prototype of the 2×2 array of four-arm curl antennas: (a) Top view, (b) Back view.

Fig. 2 shows the fabricated prototype of the array antenna. The antenna elements are excited with signals of equal amplitude and phase shifts of $\angle\beta_x$ and $\angle\beta_y$ in the x- and y-directions, respectively. The phase relationship between the ports is shown in Fig. 2. The array factor (AF) [5] of the 2×2 array can be given as:

$$AF(\theta,\phi) = \cos\left(\frac{kd\sin\theta\cos\phi + \beta_x}{2}\right)\cos\left(\frac{kd\sin\theta\sin\phi + \beta_y}{2}\right) \tag{2}$$

where k = 2π/λ_0 and d is the distance between two antenna elements. θ and ϕ are the beam direction in the elevation and azimuth planes, respectively.

III. Results

All simulations for the array in this paper are performed using Computer Simulation Technology (CST) [20]. Fig. 3 (a) shows the reflection coefficients of the array when only port A_1 is excited, and the remaining ports are terminated to a 50 Ω impedance. The port provides a reflection coefficient bandwidth of 25.7% (4.75 GHz- 6.15 GHz) for a $|S_{11}| \leq -10$ dB criterion. The S-parameters measurements are done by using four ports ZVA40 vector network analyser [21] as shown in Fig. 3(a). The measured results are in good agreement with the simulated results. It is found that the mutual couplings between port A_1 and ports B_1, C_1 and D_1 are small: less than −17.6 dB across the entire frequency test band (5 GHz – 5.3 GHz).

Fig. 4(a) and (b) show the curl antenna element radiation patterns when A_1 port is excited (other ports terminated by 50 Ω). It is found that the antenna element generates a tilted RHCP beam (θ_{max} = 48°) with a gain of 8.3 dBic. By switching the

This article has been accepted for publication in a future issue of this journal, but has not been fully edited. Content may change prior to final publication. Citation information: DOI 10.1109/LAWP.2018.2873898, IEEE Antennas and Wireless Propagation Letters

feeding ports, the curl element can provide similar RHCP beams in four different quadrants in space. The four-azimuth direction for four feed excitations of A_1, A_2, A_3 and A_4 are 210°, 300°, 30° and 120°, respectively [19].

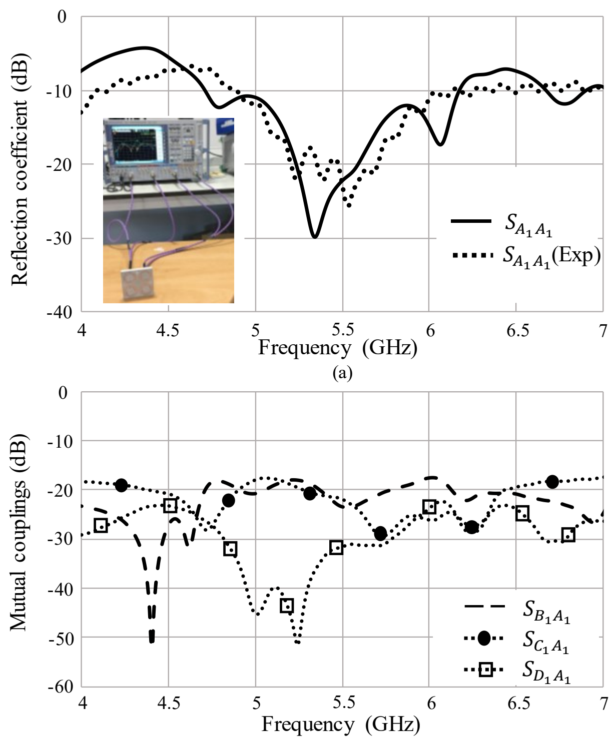

Fig. 3. S-parameters of the 2×2 array: (a) Reflection coefficient. (b) Mutual couplings.

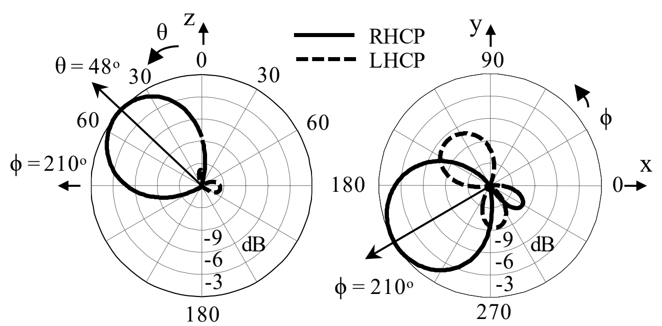

Fig. 4. Element radiation pattern of the four-arm curl antenna at 5.2 GHz: (a) Elevation plane polar cut at $\phi = 210°$ (port A_1 excited and remains ports terminated to 50 Ω). (b) Azimuth plane polar cut for port A_1 excitation at $\theta = 48°$.

In satellite communication applications, this high gain (low beam width) also has a secondary advantage of reducing the Power Flux Density (PFD) to other satellites in the geostationary arc or in other areas of the sky (e.g. for LEO (Low Earth Orbit) constellations). This is a prime consideration for terminal type approval and meeting regulatory constraints, often as important as the peak EIRP (Effective Isotropic Radiated Power) /gain criteria.

Fig. 5 shows the scanning performance of the 2×2 array in the elevation plane at $\phi = 210°$. Based on equation (2), the array provides the maximum gain of 12.4 dBic in the direction of $(\theta, \phi) = (40°, 210°)$ when the phase shifts are set to be $\angle\beta_x = 148°$ and $\angle\beta_y = 85°$. This is shown in the right side of the Fig. 5. It is found that a RHCP beam, with maximum gain of 11.6 dBic, can be steered in the direction $(\theta, \phi) = (20°, 210°)$ with phase shifts of $\angle\beta_x = 40°$ and $\angle\beta_y = 23°$. The RHCP beam maximum can be steered in the direction of $(\theta, \phi) = (70°, 210°)$ with a gain of 10.5 dBic when the phase shifts are $\angle\beta_x = 268°$ and $\angle\beta_y = 176°$. Table 1 shows the excited ports and their phase relations for achieving a full scanning range of $-80° \leq \theta \leq +80°$ (grating lobes < −12 dB and a −3 dB Gain Drop Criterion (3GDC) in the elevation plane). Furthermore, whilst a scanning range of $\theta > 80°$ is not with in the 3GDC criteria, the array is still useful in extending the coverage in some applications where there are sufficient signal margins.

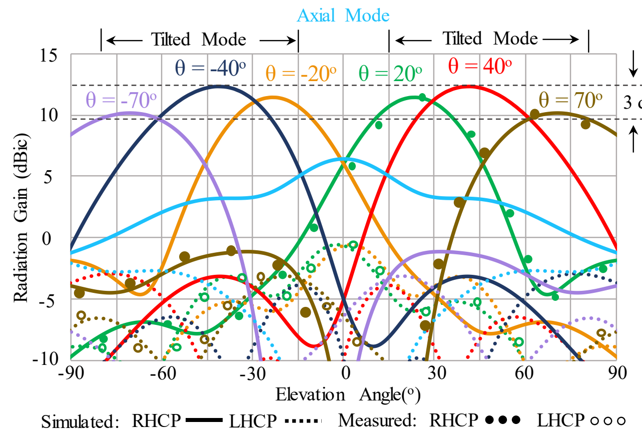

Fig. 5. Scanning range of the 2×2 curl array in the elevation plane at $\phi = 210°$, where the design frequency of 5.2 GHz is used.

TABLE I. PORT EXCITATION PHASE VALUES FOR ELEVATION PLANE SCANNING AT $\phi = 210°$ (-: NOT EXCITED)

	Tilted mode			Axial mode	Tilted mode		
θ_{max}	-70°	-40°	-20°	0°	20°	40°	70°
$\angle\beta_{A1}$	-	-	-	-	0°	0°	0°
$\angle\beta_{A2}$	-	-	-	-	-	-	-
$\angle\beta_{A3}$	0°	0°	0°	-	-	-	-
$\angle\beta_{A4}$	-	-	-	0°	-	-	-
$\angle\beta_{B1}$	-	-	-	270°	40°	148°	268°
$\angle\beta_{B2}$	-	-	-	-	-	-	-
$\angle\beta_{B3}$	-268°	-148°	-40°	-	-	-	-
$\angle\beta_{B4}$	-	-	-	-	-	-	-
$\angle\beta_{C1}$	-	-	-	-	23°	85°	176°
$\angle\beta_{C2}$	-	-	-	-	-	-	-
$\angle\beta_{C3}$	-176°	-85°	-23°	90°	-	-	-
$\angle\beta_{C4}$	-	-	-	-	-	-	-
$\angle\beta_{D1}$	-	-	-	-	63°	233°	444°
$\angle\beta_{D2}$	-	-	-	180°	-	-	-
$\angle\beta_{D3}$	-444°	-233°	-63°	-	-	-	-
$\angle\beta_{D4}$	-	-	-	-	-	-	-

Similar to [18], the array excitation has two modes. One is tilted in which same ports of each element are exited at a time (e.g. A_3, B_3, C_3 and D_3). The other mode is axial in which A_4, C_3, D_2 and B_1 are fed with the currents of equal amplitude and phase values of 0º, 90º, 180º, 270º, respectively. This yields an RHCP beam with a gain of 6.5 dBic. Interestingly, it can be noted that the array gain drops by 6 dB in the zenith. This is to the advantage as it is required when the terminal antennas operate at high latitudes for satellite communications; as at high altitudes when the GSO satellites are directly above (i.e. in the z-axis), the distance is the smallest and path loss is minimal. Hence, to avoid amplifiers going towards saturation and to maintaining a constant level of received power, the communication system requires a lower gain in this direction. For proof of concept, the measurements are performed for two beam directions of (θ = 20º and at 70º), and the experimental feeding network is shown in Fig. 6.

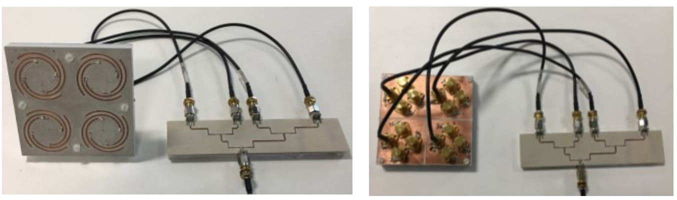

(a) (b)

Fig. 6. Measurement set-up for the maximum beam in the direction of (θ, ϕ) = (70º, 210º).

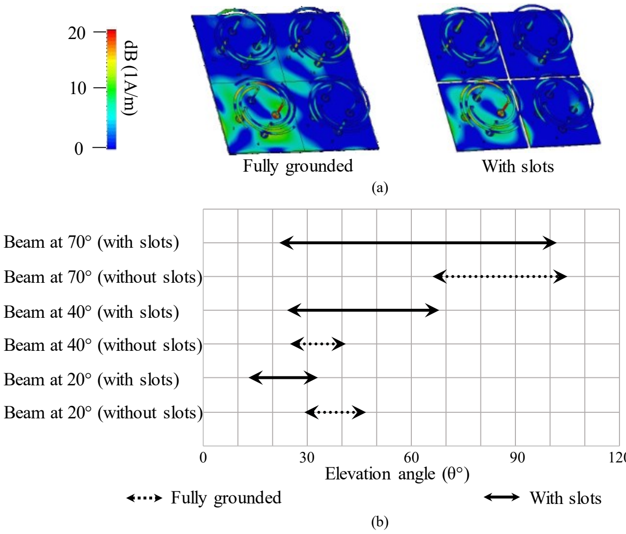

Fig. 7. Slot effect on the curl array. (a) Current distribution on the ground plane. (b) 3-dB axial ratio beam width at different directions.

Fig. 7 shows the importance of the slots cut in the ground plane for broadening the RHCP beam width. In the absence of any slot (W_S = 0), there are travelling currents on the ground plane in the diagonal direction, causing mutual coupling to neighboring elements, as seen from the current distribution in Fig. 7(a). The slots in the ground plane significantly reduce the travelling currents, which minimize the coupling effects between array elements. In absence of any slots (Fully grounded) the 3 dB axial ratio beam widths at θ = 20°, 40° and 70° are 16°, 16° and 39°, respectively. In comparison, with slots the axial ratio beam widths for θ = 20º, 40º, and 70º increase to 20º, 44º, and 80º, respectively (i.e. nearly doubled for θ = 40º and θ = 70º). We selected W_S = 1.6 mm for our design. This is the most optimized value for yielding a wide RHCP beam width with a gain of more than 10 dBic. Since the axial mode exploits circular symmetry, the polarization performance is unaffected by the slots.

Fig. 8(a) shows the frequency response of the axial ratio. It is observed that the axial ratio bandwidth (AR ≤ 3 dB) for θ = 20º, 40º, 70º are 300 MHz, 700 MHz and 400 MHz, respectively. In addition, the array provides a nearly constant realized gain for each beam direction across the AR bandwidth (Fig. 8(b)). It is also observed that the total efficiency of the array is more than 74% across the AR bandwidth without any feeding network for both the tilted and axial mode. The realized gain of the array varied from 10.8 dB to 8.4 dB for different beam positions at the test frequency. In our experiment, the phase shifting feeding network had an additional loss of 1.5 dB.

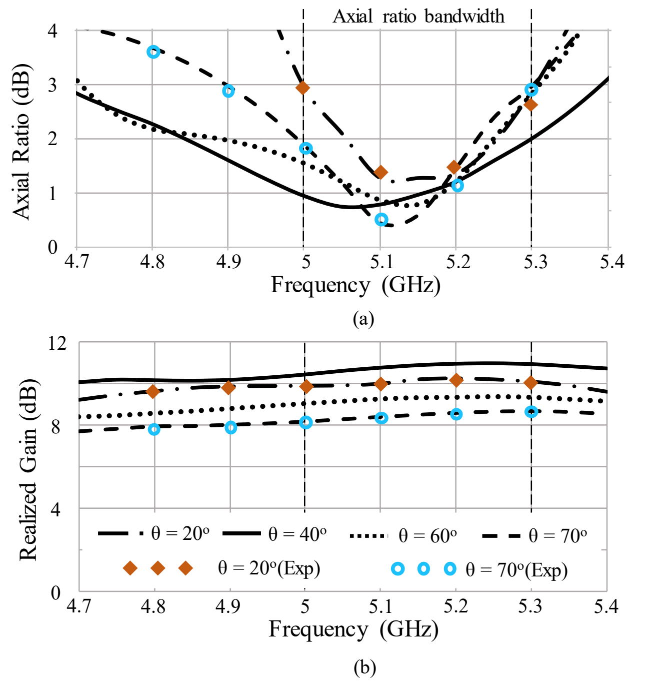

Fig. 8. Frequency response in the different maximum beam directions at ϕ = 210º. (a) Axial ratio. (b) Realized gain.

IV. Conclusion

A 2×2 array of four-arm reconfigurable curl antennas is presented for realizing near-the-horizon scanning with high-gain RHCP beams. The array operates at a design frequency of 5.2 GHz and has an effective bandwidth of 5.8% (5 GHz to 5.3 GHz). The array has two modes of operation. One tilted and one axial, and by combining them the array can scan an upper elevation plane of $-80° \leq \theta \leq +80°$. Importantly, the array provides RHCP beams with a gain of more than 10.5 dBic at near-the-horizon angles of $\theta \approx 70°$ and provides a lower gain of 6.5 dBic in the zenith direction. Therefore, the proposed array is a good candidate for mobile satellite service applications where the terminal antennas are required to have high-gain RHCP beams at low horizon angles and low gain in the zenith direction.

This article has been accepted for publication in a future issue of this journal, but has not been fully edited. Content may change prior to final publication. Citation information: DOI 10.1109/LAWP.2018.2873898, IEEE Antennas and Wireless Propagation Letters

REFERENCES

[1] R. J. Mailloux, J. F. McIlvenna, and N. Kernweis, “Microstrip array technology,” *IEEE Trans. Antennas Propag*., vol. 29, no. 1, pp. 25–37, Jan. 1981.

[2] H. Mitsumoto et al., “A mobile satellite news gathering system using a flat antenna,” *IEEE Trans. Broadcast*., vol. 42, no. 3, pp. 272–277, Sep. 1996.

[3] A. J. Fenn, D. H. Temme, W. P. Delaney, and W. E. Courtney, “The development of phased-array radar technology,” *Lincoln Lab. J.*, vol. 12, no. 2, pp. 321–340, 2000.

[4] R. C. Hansen, Phased Array Antennas, 2nd ed. New York, NY, USA: Wiley, 2009.

[5] C. A. Balanis. “Arrays: linear, Planar and Circular,” In *Antenna Theory: Analysis and Design*, 3rd ed. Hoboken, NJ, USA: Wiley, 2005. pp. 283-371.

[6] C. Liu *et al.,* “Circularly polarized beam-steering antenna array with butler matrix network,” *IEEE Antennas Wireless Propag. Lett*., vol. 10, pp. 1278–1281, Nov. 2011.

[7] S. Karamzadeh, V. Rafii, M. Kartal and B.S. Virdee, “Modified circularly polarised beam steering array antenna by utilised broadband coupler and 4 × 4 butler matrix,” *IET Microwaves, Antennas Propag.,* vol. 9, no. 9, pp. 975-981, Jun. 2015.

[8] R. Wang, B.-Z. Wang, X. Ding, and X.-S. Yang, “Planar phased array with wide-angle scanning performance based on image theory,” *IEEE Trans. Antennas Propag*., vol. 63, no. 9, pp. 3908–3917, Sep. 2015.

[9] S. E. Valavan, D. Tran, A. G. Yarovoy and A. G. Roederer, “Planar Dual-Band Wide-Scan Phased Array in X-Band,” *IEEE Trans.Antennas Propag.* vol. 62, no. 10, pp. 5370-5375, Oct. 2014.

[10] Y. Hao and C. G. Paini, “Isolation enhancement of anisotropic UC-PBG microstrip diplexer patch antenna,” *IEEE Antennas Wireless Propag. Lett.,* vol. 1, no. 1, pp. 135–137, Jan. 2002.

[11] T. A. Lam, D. C. Vier, J. A. Nielsen, C. G. Parazzoli and M. H. Tanielian, "Steering Phased Array Antenna Beams to the Horizon Using a Buckyball NIM Lens," in *Proceedings of the IEEE*, vol. 99, no. 10, pp. 1755-1767, Oct. 2011.

[12] F. Sun, and S. He, “Extending the scanning angle of a phased array antenna by using a null-space medium,” *Sci. Rep.*, vol. 4, pp. 6832, Oct. 2014.

[13] A. G. Toshev, "Multipanel Concept for Wide-Angle Scanning of Phased Array Antennas," in *IEEE Transactions on Antennas and Propagation*, vol. 56, no. 10, pp. 3330-3333, Oct. 2008.

[14] X. Ding, B.-Z. Wang, and G.-Q. He, “Research on a millimeter-wave phased array with wide-angle scanning performance,” *IEEE Trans. Antennas Propag*., vol. 61, no. 10, pp. 5319–5324, Oct. 2013.

[15] Z. Li, D. Rodrigo, L. Jofre, and B. A. Cetiner, “A new class of antenna array with a reconfigurable element factor,” *IEEE Trans. Antennas Propag*., vol. 61, no. 4, pp. 1947–1955, Apr. 2013.

[16] Y. Y. Bai, S. Q. Xiao, M. C. Tang, Z. F. Ding, and B.-Z. Wang, “Wide angle scanning phased array with pattern reconfigurable elements,” *IEEE Trans. Antennas Propag*., vol. 59, no. 11, pp. 4071–4076, Nov. 2011.

[17] S. Xiao, C. Zheng, M. Li, J. Xiong, and B. Z. Wang, “Varactor loaded pattern reconfigurable array for wide-angle scanning with low gain fluctuation,” *IEEE Trans. Antennas Propag*., vol. 63, no. 5, pp. 2364–2369, May 2015.

[18] A. Pal, A. Mehta, D. Mirshekar-Syahkal, and H. Nakano, “2 × 2 Phased Array Consisting of Square Loop Antennas for High Gain Wide Angle Scanning with Low Grating Lobes,” *IEEE Trans. Antennas Propag.*, vol. 65, no. 2, pp. 576-583, Dec. 2016.

[19] H. Zhou, A. Pal, A. Mehta, D. Mirshekar-Syahkal, and H. Nakano, “A Four-arm Circularly Polarized High-gain High-tilt Beam Curl Antenna for Beam Steering Applications,” *IEEE Antennas Wireless Propag. Lett.,* vol. 17, no. 6, pp. 1034-1038, Jun. 2018.

[20] CST Computer Simulation Technology GmbH, Darmstadt, Germany. *Microwave Studio*. accessed Jun. 2018, [Online]. Available: http://www.cst.com.

[21] Rohde & Schwarz ZVA 40 Vector Network Analyser 4 ports, Harvest Cres, United Kingdom. *Rohde & Schwarz*. accessed Jun. 2018, [Online]. Available:https://www.rohde-schwarz.com/uk/product/zva-productstartpage_63493-9660.html.